JCTC Journal of Chemical Theory and Computation

Vibronic Quasi-Free Rotation Effects in Biphenyl-Like Molecules. TD−DFT Study of Bifluorene†

Rémy Fortrie‡ and Henry Chermette*,§

Université de Lyon, École Normale Supérieure de Lyon, Laboratoire de Chimie, UMR 5182 du CNRS, 46 Allée d'Italie, F-69364 Lyon Cedex 07, France, and Université Lyon 1 and CNRS UMR 5180 du CNRS Sciences Analytiques, Chimie Physique Théorique, Bat. Paul Dirac (210), 43 Boulevard du 11 Novembre 1918, F-69622 Villeurbanne Cedex, France

Received December 19, 2006

Abstract: In this paper, we investigate the vibronic shape of the lowest UV−visible absorption band of biphenyl-like systems, using the bifluorene molecule as a workhorse. The molecule is here regarded as a one-dimensional two-level system, whose ground and excited states are simulated with time-dependent density functional theory and semiempirical methods. The vibrational Schrödinger equation is then numerically solved along the torsional coordinate, and the vibronic shape of the absorption band is modeled. Comparisons with the harmonic approximation, with or without the Franck−Condon approximation, are performed. This study confirms that a vibronic effect is most likely responsible for the strong dissymmetry of the lowest UV−visible absorption band of biphenyl-like systems and that, for such systems, the experimental data should be extracted using the whole absorption band, instead of a Gaussian fit on the first part of the band, as it is often done when a superposition between several electronic transitions is suspected.

1. Introduction

Biphenyl-like molecules belong to a class of systems that are susceptible, if steric effects do not hinder $\pi-\pi$ couplings, to easily undergo quasi-free rotation between fragments.[1−3] They also have the particularity of exhibiting a quasi-planar structure in their electronic ground state and a quasi-orthogonal structure in their first excited state.[4] Additionally, they often exhibit a significantly asymmetric lowest UV−vis absorption band, whose origin is questionable. This asymmetry can indeed be interpreted as the result of the superposition of a few electronic transitions, or as the result of a vibronic effect. This article focuses on the analysis of the origin of this asymmetry, using the bifluorene molecule as a workhorse.

Fluorene-based molecules and oligomers have indeed previously been shown to exhibit very promising nonlinear optical properties.[5−8] As a consequence, this family of compounds is of great interest for new technologies, and several experimental and theoretical investigations have already been dedicated to them.[9−13] A part of these studies consists in comparing the information resulting from both approaches. Such comparisons are however not obvious, and even if some effort has already been done for rationalizing them,[14,15] some assumptions and questions remain unjustified or unanswered.

In this article, we focus our attention on the linear optical properties of the smallest fluorene oligomer. The experimental UV−visible absorption spectrum of one of its derivatives, bi-9,9-dihexylfluorene, has already been measured[12] and modeled on the basis of an electronic approach.[8,12] Both of the previous papers focus on the lowest absorption band of the bi-9,9-dihexylfluorene molecule. The way this band is integrated is not detailed in the first paper, and in the second paper, it has been assumed that it only

† Dedicated to Professor Dennis R. Salahub on the occasion of his 60th birthday.

* Corresponding author phone: +33 4 72 44 84 27; fax: +33 4 72 44 53 99; e-mail: henry.chermette@univ-lyon1.fr.

‡ École Normale Supérieure de Lyon.

§ Université Lyon 1.

10.1021/ct600369b CCC: $37.00
Published on Web 04/19/2007

Table 1. Electronic Excitation Spectra of the Bifluorene Molecule in the Gas Phase (A//B Indicates that the Geometry Optimization has been Performed at Level B and the Excitation Spectrum Calculation at Level A)[a]

	CNDO/s//AM1[5]		ZINDO//AM1		TD-B3LYP		TD-PW91	
excited state	ΔE	f	ΔE	f	ΔE	f	ΔE	f
1	33 822	1.59	29778	1.39	30 663	1.33	26 735	1.06
2	34 334	0.01	33 237	0.01	35 346	0.00	28 928	0.00
3	34 832	0.02	33 359	0.01	35 675	0.00	30 532	0.00
4	35 543	0.00	33 908	0.00	36 051	0.00	31 049	0.00
5	35 700	0.04	34 786	0.00	37 844	0.00	32 365	0.00
6	37 809	0.03	34 960	0.00	37 918	0.00	32 482	0.01
7	40 541	0.00	39 482	0.06	38 260	0.03	34 149	0.00
8	42 961	0.05	41 472	0.02	40 830	0.00	34 165	0.00
9	45 782	0.02	42 129	0.01	41 081	0.00	35 232	0.04
10	45 805	0.15	42 956	0.08	42 139	0.05	35 291	0.03
11	46 224	0.08	42 979	0.73	42 483	0.03	35 702	0.00
12	46 555	0.00	44 151	0.12	42 813	0.18	36 384	0.28
13	46 834	0.39	44 196	1.47	43 460	0.02	36 760	0.01
14	47 018	0.17	44 498	1.16	43 765	0.00	37 216	0.11
15	47 982	0.31	45 791	0.01	44 823	0.00	37 724	0.02
16	48 322	0.64	46 003	0.18	45 415	0.02	38 028	0.01
17	48 687	0.04	46 133	0.00	45 453	0.01	38 056	0.00
18	48 798	1.74	46 868	0.00	46 047	0.00	38 516	0.00
19	49 051	0.02	46 983	0.05	46 499	0.00	38 700	0.00
20	49 335	0.04	47 871	0.00	46 979	0.01	39 663	0.00

[a] ΔE represents the excitation wavenumber in cm^{-1} and *f* the oscillator strength. Oscillator strengths larger than 0.50 are underlined. The basis set used at TD-B3LYP and TD-PW91 levels is 6-31G*.

consists of a single electronic transition, even if it is rather large and asymmetric.

The present work completes these previous studies. First, we show, on the basis of electronic excitation spectra calculations, that the single excitation assumption is relevant. Second, we confirm, on the basis of a vibronic analysis, that the asymmetric shape of the absorption band is compatible with a vibrational origin. At first glance, these results may seem of weak importance. However, depending on the origin of the asymmetry, the way the experimental transition wavenumbers and oscillator strengths are extracted and interpreted differ, which has of course some consequences on the conclusions which might be drawn using these data. For example, a trend in the oscillator strengths extracted from the experimental absorption spectra of a series of molecules could be observed, where in fact no particular trend exists, but where the absorption bands were not integrated in a proper way.

This article does neither aim to precisely reproduce the experimental data through theoretical calculations nor pretend to reproduce the complete vibronic absorption spectra of the compound of interest. We are here only concerned with getting arguments on the proper way of using experimental absorption spectra for comparison to theoretical data.

2. Electronic Excitation Spectra

In this section, we investigate the electronic absorption spectrum of the bifluorene molecule in the gas phase thanks to several electronic excitation spectra calculation methods. In each case, the molecular geometry is fully optimized, and the existence of an energy minimum is confirmed thanks to a vibrational analysis. The default thresholds and integration grid of the software have been used and no particular numerical difficulty has been encountered. Concerning semiempirical methods, AM1[16−18] is used for optimizing the geometry, while CNDO/s[5,19,20] and ZINDO[16,21,22] are used for modeling the electronic absorption spectrum. Additionally, time-dependent density functional theory (TD−DFT) calculations are performed, first using a generalized gradient approximation functional, PW91,[16,23−25] and then a hybrid functional, B3LYP,[16,26] that has previously been shown relevant for treating such problems.[27,28] The basis set used is 6-31G*. Results are gathered in Table 1.

As can be seen, whatever the method, the lowest absorption band remains isolated. No overlap with any other intense electronic transition is expected. The closest transition whose oscillator strength is larger than 0.5 is indeed at least 13 200 cm^{-1} (ZINDO//AM1 value) higher in energy than the lowest absorption band, which is much larger than the width of the experimentally observed absorption band (Figure 1).

This result confirms the idea of a vibronic origin for the dissymmetry of the absorption band. Such a phenomenon is not unusual. For example, Brédas et al. recently investigated the dissymmetric shape of the ionization band of the bifluorene molecule on the basis of a harmonic approximation.[29] The shape that they obtained is very similar to that observed for the absorption band we are interested in. A significant difference exists however: the tail theoretically obtained for the ionization band is pretty short if compared with that experimentally observed for the absorption band.

This difference suggests that at least one of the vibrational modes of the bifluorene molecule which are affected by the electronic transition is strongly anharmonic. A good candidate is the quasi-free rotation mode corresponding to the

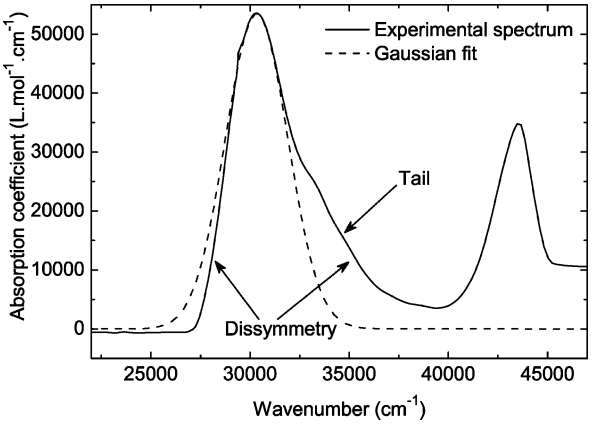

Figure 1. Experimental UV−visible absorption spectrum of bi(9,9-dihexylfluorene) in chloroform at 298 K[12] (solid line) and Gaussian approximation of the lowest absorption band fitted on the top of the band (dashed line). The parameters of the Gaussian function ($A \times \exp\{-[(x-x_C)/w]^2\}$) are $x_C = 30\,303$ cm^{-1}, $A = 53\,563$ L mol^{-1} cm^{-1}, and $w = 2277$ cm^{-1}.

respective rotation of both fluorene units. In the following sections, we investigate the consequences of the presence of such a particular vibrational mode on the shape of the lowest electronic absorption band of the bifluorene molecule.

At this point, it has to be emphasized that, from a certain point of view, the problem has here been addressed in an extreme way. Indeed, only two possibilities have been considered: either an electronic or a vibrational origin. Intermediate cases exist however. Some electronic transitions that are forbidden at the optimized geometry of the electronic ground state can indeed give rise to significant contributions if they become allowed in the vicinity of this geometry.[27] These effects are not investigated hereafter. However, since they allow the expression of electronic transitions whose transition electric dipole moments are orthogonal to the fluorene−fluorene axis or which consist of antisymmetric combinations of transitions occurring within the π systems of the fluorene units or the benzene rings, the consequences on the UV−visible absorption spectrum are expected to be either very small or located at much higher energies than that of the absorption band of interest. This assessment would of course require confirmation by calculations similar to those performed by Dierkens and Grimme,[27] which is not to be performed within the framework of this article.

3. Vibronic Spectrum

As previously mentioned, the goal of this paper is not to precisely reproduce the complete vibronic structure of the absorption spectrum of interest, but to get arguments about the way experimental data have to be extracted and used. As a consequence, and since we are here investigating the impact of the presence of the previously mentioned quasi-free rotation mode on the shape of the absorption spectrum, we will, in the next paragraphs, pay attention only to this particular motion of the molecular system. In other words, the bifluorene molecule is hereafter regarded as a one-dimensional system whose coordinate corresponds to the dihedral angle between both fluorene units ($C_aC_bC_cC_d$ dihedral angle as represented in Figure 2).

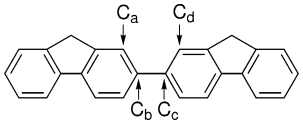

Figure 2. Bifluorene molecule. C_a, C_b, C_c, and C_d define the dihedral angle used as a coordinate for describing its internal quasi-free rotation degree of freedom.

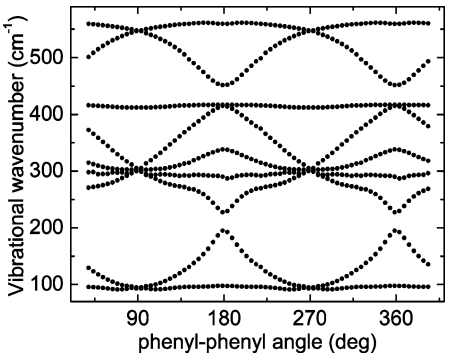

Figure 3. Wavenumbers of the softest orthogonally projected vibrational modes of the biphenyle molecule along its torsional coordinate at the B3LYP/6-31G* level of theory.

This assumption is particularly severe. First, because other vibrational modes are coupled with this torsional coordinate. This can be deduced from Figure 3, where the vibrational modes of the biphenyle molecule have been orthogonally projected with respect to its torsional coordinate. Second, because these other vibrational modes, that we are here neglecting, may also, at least partially, be responsible for the dissymmetry of the absorption band. This contribution is however expected, on the basis of previous studies[29] and on the basis of the following Franck−Condon modeling, to be weaker than the one we are here investigating.

Checking the validity of this model might be achieved by solving the vibrational Schrödinger equation of the molecular system over its 126-dimensional potential energy surface. Such a modeling is however heavily computationally demanding and then too far from the purpose of this article.

3.1. Ground State. The following levels of theory are here used for characterizing the ground state of the bifluorene molecule: AM1, B3LYP/6-31G*, B3LYP/6-311++G**,[30] and PW91/6-31G*. The previously defined torsional coordinate is sampled every 5°, starting from the fully optimized geometry. For each sample, the dihedral coordinate is frozen and all other geometric parameters are fully optimized. The corresponding energy curves are reported in Figure 4. It can be seen that the shape of the curve is independent of the level of theory and that only the sizes of the energy barriers vary, which is consistent with previous results concerning other biphenyl-like molecules.[31] It can also be seen that using additional polarization and diffuse functions does not drastically change the shape of the energy curve, and only the 6-31G* basis set is then used further in this article. Note finally that, if all methods give a similar description of the ground state potential energy curve around planar geometries (0 and 180°), there is no clear agreement around orthogonal geometries (90 and 270°), which has significant consequences on the corresponding simulated vibronic absorption spectra, as shown further in this article.

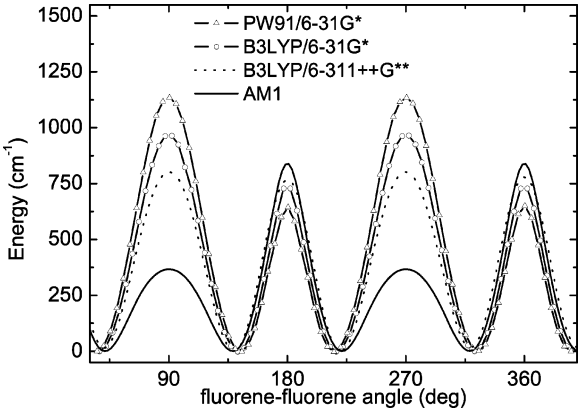

Figure 4. Ground-state energy curves of the bifluorene molecule along its torsional coordinate at the following levels of theory: AM1, B3LYP/6-31G*, PW91/6-31G*, and B3LYP/6-311++G**.[30]

3.2. Excitation Spectrum. The excitation spectrum of the bifluorene molecule is computed vertically along the torsional coordinate. The following levels of theory are used: ZINDO//AM1, TD-B3LYP/6-31G*, and TD-PW91/6-31G*. The TD-B3LYP/6-31G* excitation spectrum is plotted in Figure 5a. Other excitation spectra are not plotted but are used further in the article.

As a matter of fact, all vibrational modes are also coupled in any excited state of the bifluorene molecule. The same assumptions are however used here that have been used for the ground state. Additionally, only the vertical excitation spectrum is used. This implies that any relaxation of the excited state is neglected. This assumption is acceptable with respect to the vibronic structure of the absorption band if the relaxation energy is quasi-uniform over the torsional coordinate, which we will assume here.

The fact that, from the electronic ground state, among the 20 first possible electronic excitations, only that with the lowest transition energy is probable (Table 1) remains valid whatever the value of the torsional angle between fluorene units. The orthogonal region exhibits however a particularity: at 90 and 270°, the absorbent excited state crosses a transparent state, and they simultaneously exchange their roles. This implies that, over a very short range of angle values, both states are absorbent. However, since, in this region, both states are pseudo-degenerated, they can be rotated into two new absorbent and transparent states, without any major change of the electronic excitation spectrum. Only the first excited state is then hereafter considered.

Both ground-state and excited-state energy curves have been sampled over 72 angle values (every 5°). They are here now fitted using a Fourier's series decomposition, up to the 35th order (Figure 5b).

Vibrational eigenstates are then, for both electronic states of interest, obtained by solving the one-dimensional vibrational Schrödinger equation (eq 1), where θ represents the dihedral angle between both fluorene units, as previously described, I is the quarter of the inertial momentum of the whole molecular system with respect to the line defined by the carbon atoms of both fluorene units that are bonded together (C_b and C_c), $V(\theta)$ is the potential energy function,

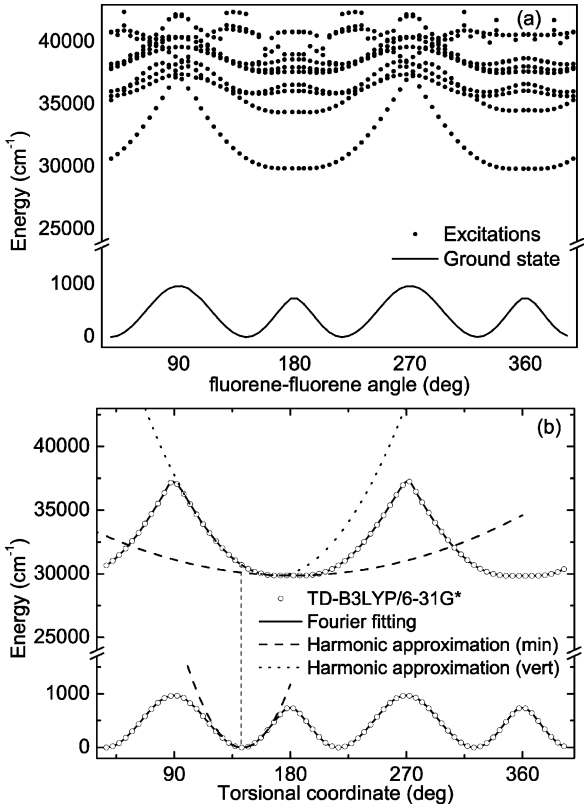

Figure 5. (a) Excitation spectrum of the bifluorene molecule along the fluorene−fluorene dihedral angle at the TD-B3LYP/6-31G* level. Solid line: ground state. Points: existing excitations, whatever the value of the corresponding transition probability. (b) Potential-energy curves associated with the ground state and with the first excited state of the bifluorene molecule along the fluorene−fluorene dihedral angle at the TD-B3LYP/6-31G* level. Empty points: sampling. Solid lines: fits obtained by Fourier decomposition up to the 35th harmonic. Dashed lines: harmonic approximations around energy minima (min). Dotted line: harmonic approximation of the first excited state vertically above the energy minimum of the ground state (vert).

$\phi(\theta)$ and E are the wave function and the energy of the system and $\hbar$ is the reduced Planck constant.

$$-\frac{\hbar^2}{2I}\frac{d^2\varphi(\theta)}{d\theta^2} + V(\theta)\,\varphi(\theta) = E\varphi(\theta) \qquad (1)$$

Since to each point of the ground-state energy curve corresponds a relaxed geometry of the molecular system, the value of I slightly depends on θ. The variation is however only about 0.8%, and the average value of 1.804×10^{-45} kg m^2 is hereafter considered (B3LYP/6-31* value). The solutions are developed on a plane waves basis set truncated at the 600th harmonic (1201 basis functions), which corresponds here to a cutoff of 55 863 cm^{-1}. Vibrational eigenstates are graphically represented on Figures 6 and 7, where it can in particular be seen that the vibrational eigenstates are well-converged.

3.3. Oscillator Strengths. The electronic part of the transition electric dipole moment between the electronic ground and excited states strongly varies along the torsional

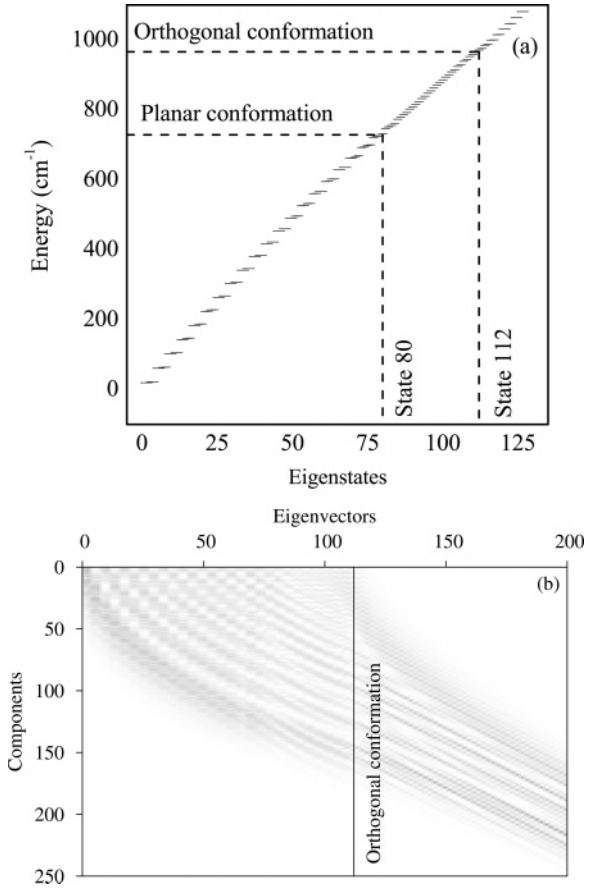

Figure 6. Vibrational eigenstates associated with the electronic ground state. (a) Eigenvalues of the vibrational Hamiltonian operator. (b) Absolute values of the components of the corresponding eigenvectors (continuous grayscale between 0:white and 1:black).

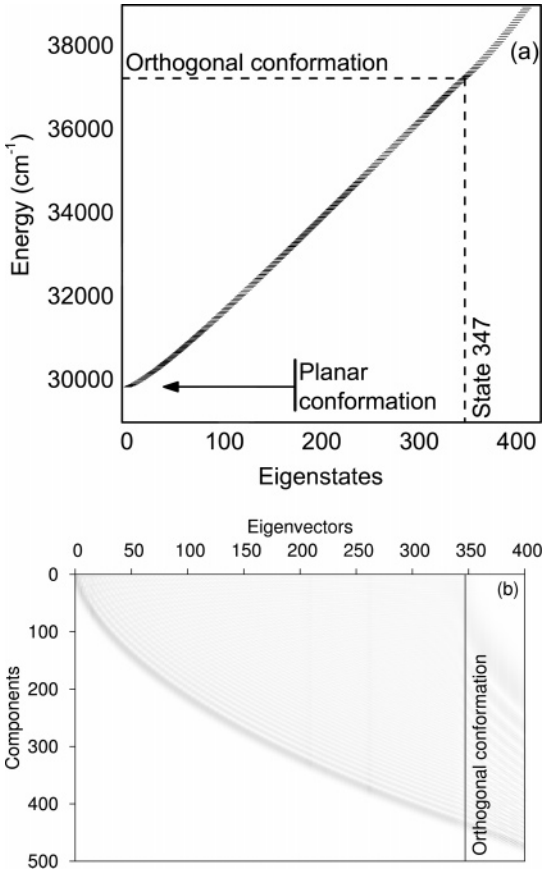

Figure 7. Vibrational eigenstates associated with the electronic excited state. (a) Eigenvalues of the vibrational Hamiltonian operator. (b) Absolute values of the components of the corresponding eigenvectors (continuous grayscale between 0:white and 1:black).

coordinate (Figure 8). As a consequence, transition electric dipole moments between vibronic states, $\langle\psi_{0,v}|\vec{\mu}|\psi_{1,v'}\rangle$, where 0 and 1 refer to the electronic ground and excited states, respectively, and v an v′ refer to the vibrational eigenstates, are numerically calculated without further approximation.

3.4. Vibronic Spectrum. A weight is finally attributed to each vibronic transition, depending on the population of the initial vibronic state at the temperature T of interest. We here assume that these populations follow a Boltzmann distribution and each weight is then equal to $\exp(-E_v/k_BT)$, where E_v is the energy of the initial vibronic state and k_B is the Boltzmann constant. The complete vibronic absorption spectrum then consists of the sum of the contributions of all weighted vibronic transitions.

4. Results

In Figure 9 are represented the resulting vibronic absorption spectra. Individual vibronic transitions have been convoluted with Gaussian functions (fwhm: 1000 cm^{-1}). As can be seen on this figure, the absorption band is dissymmetric and becomes larger and weaker when the temperature increases. This behavior is a typical vibronic effect and is also observed within the framework of a more usual harmonic approach (Figure 10).[32] In this figure, for making comparison easier, the spectra corresponding to the harmonic approximation

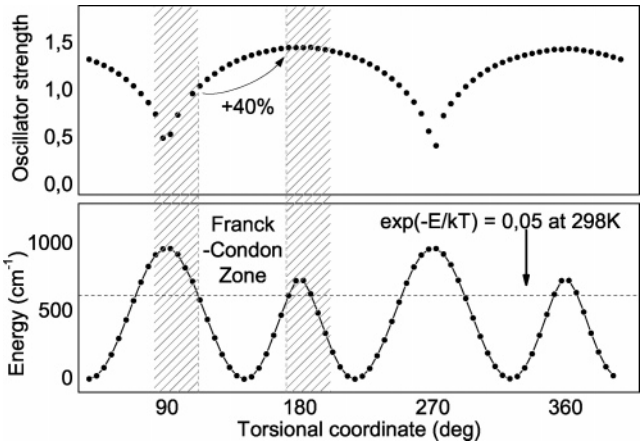

Figure 8. (Top) Oscillator strength corresponding to the electronic part of the transition electric dipole moment between the electronic ground and excited states along the torsional coordinate (B3LYP/6-31G*). (Bottom) Potential-energy curve associated with the electronic ground state (B3LYP/6-31G*). The variation of the oscillator strength over the Franck−Condon zone associated with a limiting Boltzmann factor of 0.05 at 298 K is also represented.

have been shifted and vertically scaled in such a way that the maxima of all curves match up.

As can be seen looking at both scaling factors, using the harmonic approximation leads to a slight overestimation of

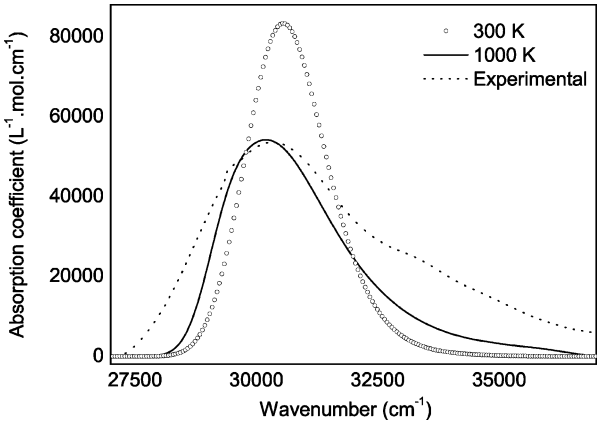

Figure 9. Vibronic absorption spectrum of the bifluorene molecule (TD-B3LYP/6-31G*). Individual vibronic transitions have been convoluted with Gaussian functions (fwhm: 1000 cm^{-1}). No scaling or shifting factor has been applied.

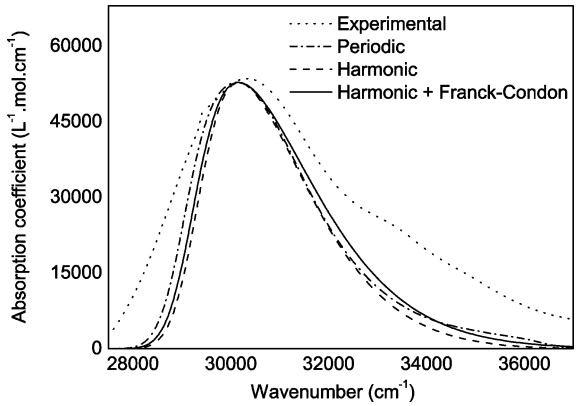

Figure 10. TD-B3LYP/6-31G* vibronic absorption spectra of the bifluorene molecule using different vibrational models: periodic or harmonic, with or without the Franck−Condon approximation.[32] Harmonic frequencies, 41.6 cm^{-1} for the ground state and 56.7 cm^{-1} for the excited state, have been obtained by derivation of the electronic potentials, with respect to the torsional angle, for the conformation corresponding to the energy minimum of the ground state (Figure 5). Harmonic and Franck−Condon approximations: shift = 25 cm^{-1}, vertical scaling factor = 89.9%. Harmonic approximation only: shift = 125 cm^{-1}, vertical scaling factor = 83.8%.

the maximum absorption coefficient. It can also be seen that the harmonic approximation fails in correctly describing both the low- and high-energy parts of the absorption band. The low-energy part is too tight and the high-energy part is too wide within the Franck−Condon approximation and falls too short without. In other words, the harmonic approximations are here inadequate for accurately describing the dissymmetry and a long high-energy tail of the absorption band. There are two reasons for this. First, the harmonic approximation simply underestimates the molecular population around orthogonal conformations, and molecules with such conformations are precisely responsible for the existence of the long high-energy tail. Second, as can be seen in Figure 5, the harmonic approximation does not correctly reproduce the potential energy curve of the excited state around planar

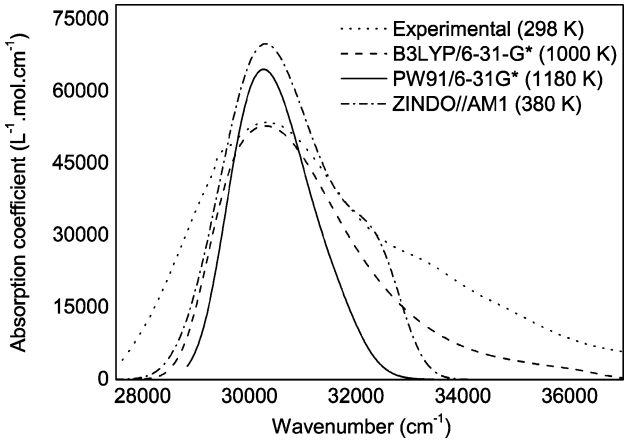

Figure 11. Vibronic absorption band modeled at different levels of theory: ZINDO//AM1 (380 K, shift = 553 cm^{-1}), and TD-PW91/6-31G* (1180 K, shift = 3833 cm^{-1}), and TD-B3LYP/6-31G* (1000 K, shift = 178 cm^{-1}).

conformations, and transitions occurring in these regions are precisely responsible for the low-energy part of the absorption band.

The reader would have noticed that the temperature for which the vibronic spectra are compared is rather high (1000 K) if compared with usual experimental temperatures (300 K). However, this temperature strongly depends on the quality of the description of the potential energy curves of both electronic states, which strongly depends on the quality of the theoretical method.

First, the electronic eigenstates have been calculated for a gas-phase bifluorene, whereas experimental data have been measured in chloroform. This has two consequences: (i) Molecular polarizabilities should be multiplied by a local field factor for any comparison with macroscopic experimental data. (ii) Chloroform is known to generate solvatochromism effects, which are here not taken into account.[33]

Second, we are here modeling the bifluorene, but experimental data concern the bi(9,9-dihexylfluorene). Whereas, electronically, replacing hexyl groups by hydrogen atoms almost has no consequence since the lowest electronic transition mainly involves the π system, it has dynamic consequences which are known to strongly affect, at least, the potential energy barriers of the electronic ground state.[30] In other words, because of the approximations contained in the sterically simplified model, the theoretical energy barrier is too high, which leads to too high temperatures necessary for modeling the dissymmetry of the spectra. It is then not surprising that the temperature value which corresponds to a particularly strong dissymmetry is experimentally unrealistic.

In order to confirm the vibronic origin of the dissymmetry of the absorption band, two other theoretical methods have been used for modeling the vibronic absorption spectrum: TD-PW91/6-31G* and ZINDO//AM1 (Figure 11). Since the high-energy tail results from the molecules whose conformations are close to the orthogonal one, and since the energy of this particular conformation strongly depends on the theoretical method, the ZINDO//AM1 and TD-PW91/6-31G* spectra have been calculated at 380 and 1180 K, respectively,

so that the Boltzmann factor corresponding to the orthogonal conformation is identical for all methods and we can easily compare the resulting spectra.

At first glance, it appears that both tails are much shorter than with the TD-B3LYP/6-31G* method. This simply comes from the fact that the energy difference between the planar and orthogonal conformations in the excited state is much smaller for ZINDO//AM1 (3357 cm^{-1}) and TD-PW91/6-31G* (3822 cm^{-1}) than for TD-B3LYP/6-31G* (7449 cm^{-1}). Deciding which value is correct is of weak importance and beyond the scope of this article. What is important here is that all three methods give rise to a strongly dissymmetric absorption band with a relatively long high-energy tail. Of course, each method gives rise to a slightly different shape. On the one hand, the TD-PW91/6-31G* method leads to a less dissymmetric and then less convincing shape, but on the other hand, the ZINDO//AM1 method gives rise to a high-energy shoulder, which is similar to that of the experimental spectrum. Anyway, as previously mentioned, it is here very difficult to decide which method gives the best result, and the reality is most probably something in between.

5. Conclusion

In conclusion, we have shown in this paper that the strong dissymmetry and the high-energy tail of the lowest electronic absorption band of the bifluorene molecule are most probably related to a vibronic effect rather than to the overlap of several electronic transitions. This can be generalized to bigger molecular systems, so that by extension, and even if no vibronic analysis has yet been performed, it is reasonable to postulate that the dissymmetric shape of the lowest electronic absorption band of other oligofluorenes is essentially due to vibronic effects.

From the results obtained within this article, it can be deduced that the electronic properties of the transitions involved in the lowest electronic absorption band of oligofluorenes should be extracted using the whole absorption band instead of a single Gaussian function fitted on the first part of the band. This legitimizes, in particular, the way these data have been extracted in a previous paper.[8]

The simple model presented in this article gave some interesting and useful information for extracting electronic data from experimental spectra. The next challenge is now of course to completely model the vibronic absorption spectra of the bifluorene molecule. However, as mentioned above, achieving such a modeling is a difficult task since the molecular system of interest contains 126 internal degrees of freedom. Moreover, the intermediate level of theory used in the present work is known to give a good physical description of common molecular systems but to poorly perform as far as numerical values concerning the electronic transitions are concerned. A more adequate level of theory, like TD-CAM-B3LYP/6-311++G**, for example, where CAM stands for Coulomb-attenuated model,[34,35] would be necessary for such a more precise modeling, making this task still more challenging.

Acknowledgment. H.C. would like to express his greatest appreciation to Dennis R. Salahub for his pioneering contributions to the development of density functional theory codes and applications to difficult problems in physical chemistry. He is also grateful to him for a long-standing collaboration. The authors are pleased to dedicate this paper to him for his 60th birthday. The authors also thank Dr. Chantal Andraud for providing them with the original file of the CNDO/s//AM1 one-photon absorption spectrum of bifluorene.

References

(1) Tachikawa, H.; Kawabata, H. *J. Phys. Chem. B* **2003**, *107*, 1113−1119.

(2) Nori-shargh, D.; Asadzadeh, S.; Ghjanizadeh, F.-R.; Deyhimi, F.; Mohammadpour, M.; Jameh-Bozorghi, S. *J. Mol. Struct.* **2005**, *717*, 41−51.

(3) Mantas, A.; Deretey, E.; Ferretti, F. H.; Estrada, M.; Csizmadia, I. G. *J. Mol. Struct.* **2000**, *504*, 77−103.

(4) Baca, A.; Rossetti, R.; Brus, L. E. *J. Chem. Phys.* **1979**, *70*, 5575−5581.

(5) Andraud, A.; Anemian, R.; Collet, A.; Nunzi, J.-M.; Morel, Y.; Baldeck, P. L. *J. Opt. A: Pure Appl. Opt.* **2000**, *2*, 284−288.

(6) Barsu, C.; Anémian, R.; Andraud, C.; Stephan, O.; Baldeck, P. L. *Mol. Cryst. Liq. Cryst.* **2005**, *446*, 175−182.

(7) Barsu, C.; Andraud, C.; Amari, N.; Spagnoli, S.; Baldeck, P. L. *J. Nonlinear Opt. Phys. Mater.* **2006**, *14*, 311−318.

(8) Fortrie, R.; Anémian, R.; Stephan, O.; Mulatier, J.-C.; Baldeck, P. L.; Andraud, C.; Chermette, H. *J. Phys. Chem. C* **2007**, *111*, 2270−2279.

(9) Reinhardt, B. A. *Photo. Sci. News* **1998**, *4*, 21−34.

(10) Cho, B. R.; Son, K. H.; Lee, S. H.; Song, Y. S.; Lee, Y. K.; Jeon, S. J.; Choi, J. H.; Lee, H.; Cho, M. H. *J. Am. Chem. Soc.* **2001**, *123*, 10039−10045.

(11) Kannan, R.; He, G. S.; Yuan, L. X.; Xu, F. M.; Prasad, P. N.; Dombroskie, A. G.; Reinhardt, B. A.; Baur, J. W.; Vaia, R. A.; Tan, L. S. *Chem. Mater.* **2001**, *13*, 1896−1904.

(12) Morel, Y.; Irimia, A.; Najechalski, P.; Kervella, Y.; Stephan, O.; Baldeck, P. L.; Andraud, C. *J. Chem. Phys.* **2001**, *114*, 5391−5396.

(13) Belfield, K. D.; Hagan, D. J.; Van Stryland, E. W.; Schafer, K. J.; Negres, R. A. *Org. Lett.* **1999**, *1*, 1575−1578.

(14) Fortrie, R.; Chermette, H. *C. R. Chim.* **2005**, *8*, 1226−1231.

(15) Fortrie, R.; Chermette, H. *J. Chem. Phys.* **2006**, *124*, 204104.

(16) Frisch, M. J.; Trucks, G. W.; Schlegel, H. B.; Scuseria, G. E.; Robb, M. A.; Cheeseman, J. R.; Montgomery, J. A., Jr.; Vreven, T.; Kudin, K. N.; Burant, J. C.; Millam, J. M.; Iyengar, S. S.; Tomasi, J.; Barone, V.; Mennucci, B.; Cossi, M.; Scalmani, G.; Rega, N.; Petersson, G. A.; Nakatsuji, H.; Hada, M.; Ehara, M.; Toyota, K.; Fukuda, R.; Hasegawa, J.; Ishida, M.; Nakajima, T.; Honda, Y.; Kitao, O.; Nakai, H.; Klene, M.; Li, X.; Knox, J. E.; Hratchian, H. P.; Cross, J. B.; Bakken, V.; Adamo, C.; Jaramillo, J.; Gomperts, R.; Stratmann, R. E.; Yazyev, O.; Austin, A. J.; Cammi, R.; Pomelli, C.; Ochterski, J. W.; Ayala, P. Y.; Morokuma, K.; Voth, G. A.; Salvador, P.; Dannenberg, J. J.; Zakrzewski, V. G.; Dapprich, S.; Daniels, A. D.; Strain, M. C.; Farkas, O.; Malick, D. K.; Rabuck, A. D.; Raghavachari, K.; Foresman, J. B.; Ortiz, J. V.; Cui, Q.; Baboul, A. G.; Clifford, S.; Cioslowski, J.; Stefanov, B. B.; Liu, G.; Liashenko, A.;

Piskorz, P.; Komaromi, I.; Martin, R. L.; Fox, D. J.; Keith, T.; Al-Laham, M. A.; Peng, C. Y.; Nanayakkara, A.; Challacombe, M.; Gill, P. M. W.; Johnson, B.; Chen, W.; Wong, M. W.; Gonzalez, C.; Pople, J. A. *Gaussian 03*, revision B.05; Gaussian, Inc.: Wallingford, CT, 2003.

(17) Dewar, M. J. S.; Thiel, W. *J. Am. Chem. Soc.* **1977**, *99*, 2338−2339.

(18) Dewar, M. J. S.; Zoebisch, E. G.; Healy, E. F.; Stewart, J. J. P. *J. Am. Chem. Soc.* **1985**, *107*, 3902−3909.

(19) Baumann, H. *QCPE Bull.* **1977**, *11*, 333.

(20) Ziegler, L.; Albrecht, A. C. *J. Chem. Phys.* **1974**, *60*, 3558−3561.

(21) Zerner, M. C.; Correa de Mello, P.; Hehenberger, M. *Int. J. Quantum Chem.* **1982**, *21*, 251−257.

(22) Zerner, M. C. In *Rev. Comp. Chem.*; Zerner, M. C., Lipkowitz, K. B., Boyd, D. B., Eds.; VCH Publishing: New York, 1991; Vol. 2, pp 313−365.

(23) Perdew, J. P. In *Electronic Structure of Solids '91*; Ziesche, P., Eschrig, H., Eds.; Akademie Verlag: Berlin, 1991; Vol. 91, Chapter 11.

(24) Perdew, J. P.; Chevary, J. A.; Vosko, S. H.; Jackson, K. A.; Pederson, M. R.; Singh, D. J.; Fiolhais, C. *Phys. Rev. B: Condens. Matter Mater. Phys.* **1992**, *46*, 6671−6687.; *Phys. Rev. B: Condens. Matter Mater. Phys.* **1993**, *48*, 4978−4978.

(25) Perdew, J. P.; Burke, K.; Wang, Y. *Phys. Rev. B: Condens. Matter Mater. Phys.* **1996**, *54*, 16533−16539.

(26) Becke, A. D. *J. Chem. Phys.* **1993**, *98*, 5648−5652.

(27) Dierkens, M.; Grimme, S. *J. Chem. Phys.* **2004**, *120*, 3544−3554.

(28) Sánchez-Carrera, R. S.; Coropceanu, V.; da Silva Filho, D. A.; Fiedlein, R.; Osikowicz, W.; Murdey, R.; Suess, C.; Salaneck, W. R.; Brédas, J.-L. *J. Phys. Chem. B* **2006**, *110*, 18904−18911.

(29) Coropceanu, V.; André, J.-M.; Malagoli, M.; Brédas, J.-L. *Theor. Chem. Acc.* **2003**, *110*, 59−69.

(30) Marcon, V.; van der Vegt, N.; Wegner, G.; Raos, G. *J. Phys. Chem. B* **2006**, *110*, 5253−5261.

(31) Sancho-Carcía, J. C. *J. Chem. Phys* **2006**, *124*, 124112.

(32) Wilson, E. B., Jr.; Decius, J. C.; Cross, P. C. *Molecular Vibrations*; Dover Publications: Mineola, NY, 1980; p 14.

(33) Machado, C.; Machado, V. G. *J. Chem. Educ.* **2001**, *78*, 649−651.

(34) Yanai, T.; Tew, D. P.; Handy, N. C. *Chem. Phys. Lett.* **2004**, *393*, 51−57.

(35) Baev, A.; Salek, P.; Gel'mukhanov, F.; Ågren, H. *J. Phys. Chem. B* **2006**, *110*, 5379−5385.

CT600369B